Structural Characterization of Nickel Oxide

V. Massarotti, D. Capsoni, V. Berbenni, R. Riccardi, and A. Marini

Dipartimento di Chimica Fisica dell'Università di Pavia and
C.S.T.E. C.N.R. – Pavia (Italy)

E. Antolini

Ansaldo SpA, Divisione Ricerche, corso Perrone 25, 16161 Genova

Z. Naturforsch. **46 a,** 503–512 (1991); received March 25, 1991

It is known from the literature that a slight distortion of the ideal cubic cell is present in the NiO structure. This work shows that such a distortion can be accurately evaluated by means of a refinement of the structural and profile parameters of X-ray powder diffraction data. Moreover, since only small amounts of products are sometimes at disposal to perform structural characterizations, it was thought useful to extend the refinement procedure to X-ray data collected on NiO samples of much lower mass (15–60 mg) than those usually utilized in X-ray diffractometric studies. The results obtained show that reliable structural parameters can be obtained from low mass samples too.

Key words: X-ray powder diffraction, Structural and profile refinement, Low mass samples, Nickel oxide.

1. Introduction

It is well known that both deviations from stoichiometry [1–3] and doping with aliovalent cations [4, 5] can be responsible of the semiconducting properties of nickel oxide. The electrical [3, 6] and magnetic [7] properties of different materials based on nickel oxide, particularly solid solutions of the type $Li_xNi_{1-x}O$, have been extensively studied. These compounds are now in use in the construction of electromagnetic and electrochemical devices [8–10], so there is a great deal of interest on them.

Structural studies based on X-ray powder diffraction were performed on NiO [11], $LiNiO_2$ and $NaNiO_2$ [12] and on some solid solutions of the type $Li_xNi_{1-x}O$ [7]. All these studies agree in indicating the presence in the NiO structure of a small distortion of the ideal cubic cell. According to [11], in which such a distortion was reported for the first time, the structure at room temperature can be described by a primitive rhombohedral cell characterized by $a' = 2.9518$ Å and $\alpha' = 60.07°$. However the distortion is so small that it generates appreciable splitting of the reflexions only at high angle values.

According to the common crystallographic use, the space group based on the rhombohedral Bravais lattice can be treated both with hexagonal and rhombohedral axes. The former are generally preferred due to the easier structure visualization they make possible. The lattice parameters a and c of the triple hexagonal cell are related to the parameters a' and α' of the primitive rhombohedral cell by [13]

$$a = 2a' \sin(\alpha'/2), \tag{1}$$

$$c = a' [3(1 + 2\cos\alpha')]^{1/2}, \tag{2}$$

and their values are $a = 2.9549$ Å and $c = 7.2266$ Å. The hexagonal cell can also be directly referred to the cubic cell: the c axis of the former will be along the direction of the diagonal of the latter. As a consequence, the family of planes constituted by alternate layers of nickel and oxygen ions, which are indicated by the Miller indices hhh with respect to the cubic axes, will be described as 001 planes with respect to the hexagonal axes. The a axis of the hexagonal prism lies on the diagonal of a face of the cube and its length is one half of the length of the diagonal itself. In the absence of any distortion one will have (a_c is the cubic lattice constant)

$$a = a_c/\sqrt{2}, \quad c = a_c \cdot \sqrt{3}, \tag{3}$$

$$c/a = \sqrt{6} = 2.44949\,. \tag{4}$$

If a rhombohedral distortion is present, one must expect that the c/a ratio deviates from its theoretical value.

Reprint request to Prof. V. Massarotti, Dipartimento di Chimica Fisica dell'Università di Pavia, viale Taramelli 16, 27100 Pavia (Italy).

0932-0784 / 91 / 0600-0503 $ 01.30/0. – Please order a reprint rather than making your own copy.

The first aim of the present work is to see if the structural distortion (c/a) of nickel oxide can be accurately evaluated by refinement of the structural and profile parameters of X-ray powder diffraction data. The second aim is to verify if such a method can be reliably applied to low mass samples (15–60 mg), i.e. to samples of much lower mass than those usually employed to collect diffractometric X-ray data on powders. The results of this study might be of remarkable usefulness, as it would be highly desirable to perform structural characterizations on samples of well defined and controlled composition as those prepared, under controlled conditions, but on a scale of few tens of a milligram, on a thermobalance.

2. Experimental

2.1. Products

Nickel oxide was obtained by oxidation, in air, of the nickel powder INCO 255. The powder was heated (heating rate 1 °C/min) up to 850 °C, then maintained at this temperature for 24 h to assure complete oxidation. Two micrographs of the product so obtained are shown in Fig. 1 (micrographs were collected on gold sputtered samples with a scanning electron microscope Cambridge Stereoscan 200).

2.2. Apparatus and Procedures

2.2.1. Diffractometric Measurements

Diffractometric measurements were performed by means of a Philips PW 1710 powder diffractometer, equipped with a vertical goniometer Philips PW 1050 and with a graphite bent crystal monochromator. Use was made of the CuKα radiation ($K\alpha_1 = 1.5406$ Å, $K\alpha_2 = 1.5443$ Å). Powder patterns were taken in the angular range 35–154° (2Θ) in step scan made with a counting time of 0.3 s/step and step widths of 0.02, 0.03, 0.05, 0.10, 0.15°. Measurements were performed both on "bulk" samples (sample mass 1–2 g), backpressed into an aluminum sample holder, and on thin layer samples (sample mass 15–60 mg, layer thickness about 0.1 mm, in the following referred to as "low mass samples") prepared by dispersing the powder between two polyethylene films.

2.2.2. Rietveld Refinement Procedure

The refinement of the structural and profile parameters, based on the comparison of the calculated patterns with the experimental ones [14], was performed with the program DBW 3.2 S [15], to which reference should be made also for what concerns its general description and the meaning of the discrepancy factors quoted below. The calculations were performed both for the hexagonal (S.G. R-3 m) and for the cubic (S.G. Fm3m) cell. The following atomic coordinates were used: a) Ni (0, 0, 0), O (0, 0, 1/2); b) Ni (0, 0, 0), O (1/2, 1/2, 1/2). The atomic scattering factors of the Ni^{2+} and O^{2-} ions were taken from [16] and [17], respectively.

The refinement procedure consisted of the following steps:

1) refinement of the scale factor, of the zero error and of a background coefficient independent of the angle (3 variable parameters);
2) refinement of the lattice parameters a and c together with the previous parameters (5 variable parameters);
3) refinement of three more background parameters dependent on the angle [15], for a total of 8 variable parameters;
4) refinement of an asymmetry parameter [14, 15] and of three peak profile parameters by means of the pseudo Voigt function [18, 19]: of these three two are related to the full width at half maximum (FWHM) of the Gaussian component [one angle dependent (u) and one angle independent (w)], while the third (y) describes the dependence of the FWHM on the Lorentzian component;
5) refinement of two isotropic thermal parameters, B(Ni) and B(O) which, added to the parameters included in the previous steps, led to a total of 14 variable parameters refined in this step.

Each step was considered to converge when the difference between the values of the variable parameters obtained in two successive cycles was lower than 0.3 e.s.d. (estimated standard deviation). The values of the variable parameters obtained by each step were used as initial values for the successive step.

3. Results and Discussion

3.1. "Bulk" Samples

The result of the refinement performed on the basis of the hexagonal cell are reported in the first column of Table 1 (initial values of the lattice parameters: $a = 2.9549$ Å; $c = 7.2266$ Å). Exactly the same results were obtained starting with the cubic parameter,

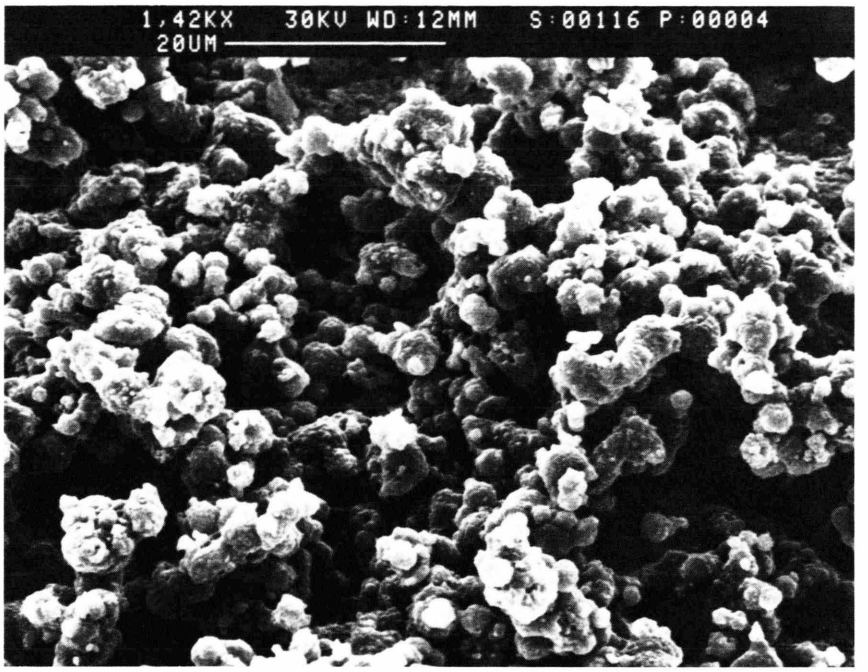

(a)

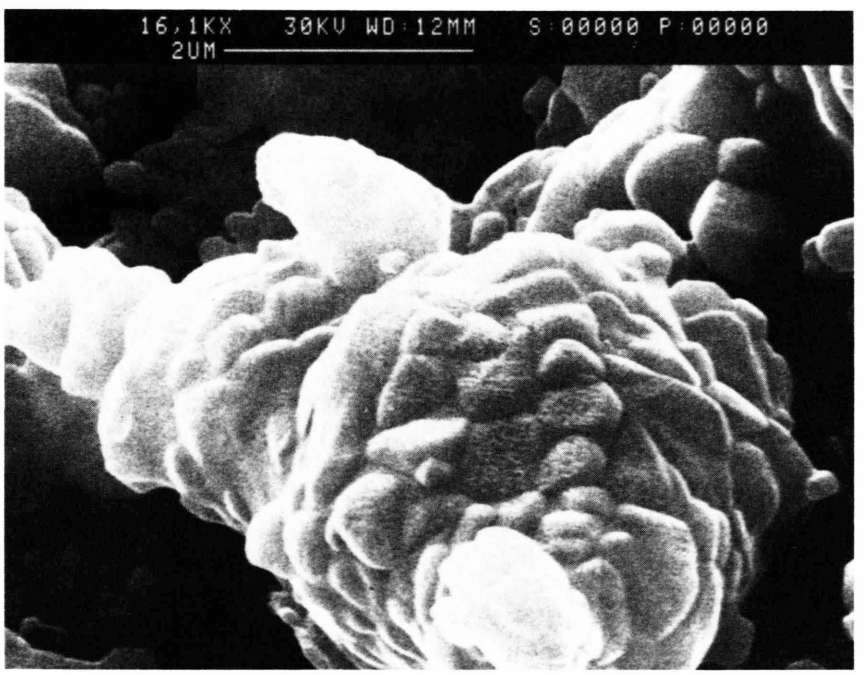

(b)

Fig. 1. Low (a) and high (b) magnification micrographs of a sample of the NiO powder prepared as described in the experimental section.

Table 1. Refined parameters obtained by applying different models to X-ray data collected on a "bulk" sample under the following conditions: step width = 0.02°; step counting time = 0.3 s; filament current = 35 mA. N and $\sum y_i$ represent the total number of steps and the total counts of the pattern, respectively. See the text for a full description of the different models.

	Model 1 Hexagonal	Model 2 Hexagonal	Model 3 Cubic
B (Ni)	0.3159	0.3670	0.3649
	159	186	188
B(O)	0.3068	0.4342	0.4269
	443	528	533
Scale · 10^2	0.341	0.343	0.386
	17	20	22
u	0.00333	0.01654	0.02168
	31	99	56
w	0.00377	0.00215	0.00160
	16	23	22
y	0.04314	0.04250	0.04262
	90	101	101
$a = b$	2.95449	2.95239	4.17646
	2	5	4
c	7.22641	7.23786	–
	7	27	
Asymm.	0.88162	0.84363	0.78837
	7223	8272	8035
Zero	0.0339	0.0361	0.0359
	5	6	6
R_p	8.82	10.76	10.96
R_{wp}	12.20	14.14	14.30
R_E	10.47	10.47	10.47
GoF	1.36	1.82	1.86
D	1.59	1.26	1.24
R_B	2.25	2.97	2.51
R_F	1.28	2.12	1.40
c/a	2.44591	2.45152	–
	8	27	
$\frac{\sum y_i}{N} \cdot 10^{-6}$	0.4146	0.4146	0.4146
	4549	4549	4549
Q	1.91	1.91	1.91

transforming it into hexagonal parameters via (3), and then applying a slight distortion (up to 0.07%). The initial value of the cubic parameter (4.17563 Å) was obtained by the linear regression method from the angular positions of the observed reflexions. The corresponding undistorted hexagonal parameters were: $a = 2.95262$ Å and $c = 7.23241$ Å. With an 0.07% expansion for a and contraction for c, the following lattice parameters were obtained: $a = 2.9547$ Å, $c = 7.2274$ Å, which were used as initial values in the refinement. In this case too, the final values of the lattice parameters were: $a = 2.95449(2)$ Å and $c = 7.22641(7)$ Å. The c/a ratio ($c/a = 2.44591(8)$) shows a slight but appreciable distortion.

A refinement was also performed with initial values of the lattice parameters obtained by applying an opposite distortion (contraction of a and expansion of c) to the hexagonal parameters obtained as explained above. The results are reported in the second column of Table 1, while the comparison between the pattern observed and those calculated from both refinements is shown in Figure 2. In order to understand the differences between the two treatments, it appears particularly important to compare the refined parameters u, w, y. The first two of them describe the angular dependence of the Gaussian component [$HG = (u\,\mathrm{tg}^2\,\Theta + w)^{1/2}$] of the FWHM, while the third one describes the behaviour of the width of the Lorentzian component [$HL = y/\cos\Theta$] of the profile. Table 1 shows that the coefficients of the Gaussian component change appreciably on passing from the first to the second kind of refinement. In the latter one the Gaussian width results increased appreciably, as it can be seen from the curves HG-I and HG-II of Fig. 3, while the Lorentzian width remains substantially unchanged (curves HL-I and HL-II of Figure 3). As a consequence, the total FWHM is much higher in the second refinement than in the first one. A comparison between the experimental and calculated patterns for the high angle reflexions is reported, for both refinements, in Figure 4. It can be seen that the difference between the observed and calculated patterns becomes appreciable for the second refinement, leading to an appreciable increase of the discrepancy, factors and of the goodness of the fit that such a refinement presents over the first one (see Table 1). Moreover, as a consequence of the increased FWHM, no separation is possible in the calculated profile of the second refinement, of the reflexions 300, 214 and 018 which, on the contrary, result separated both in the pattern calculated according to the first refinement and in the observed one. Experimental evidence then indicates that the first model, whose c/a ratio is lower than $\sqrt{6}$, is much more reliable than the second one ($c/a > \sqrt{6}$).

A refinement was also started, based on an undistorted hexagonal model; however the second step of the refinement procedure failed to converge, so that no result is reported in Table 1 for such a model. Convergence was on the contrary obtained in all the steps of the described procedure for a refinement based on a cubic model. The results obtained in this case, which obviously cannot explain the observed separation of the high angle reflexions, are reported in the third column of Table 1. The discrepancy factors are higher than those obtained for the first hexagonal model. Thus, only the use of a slightly distorted hexagonal

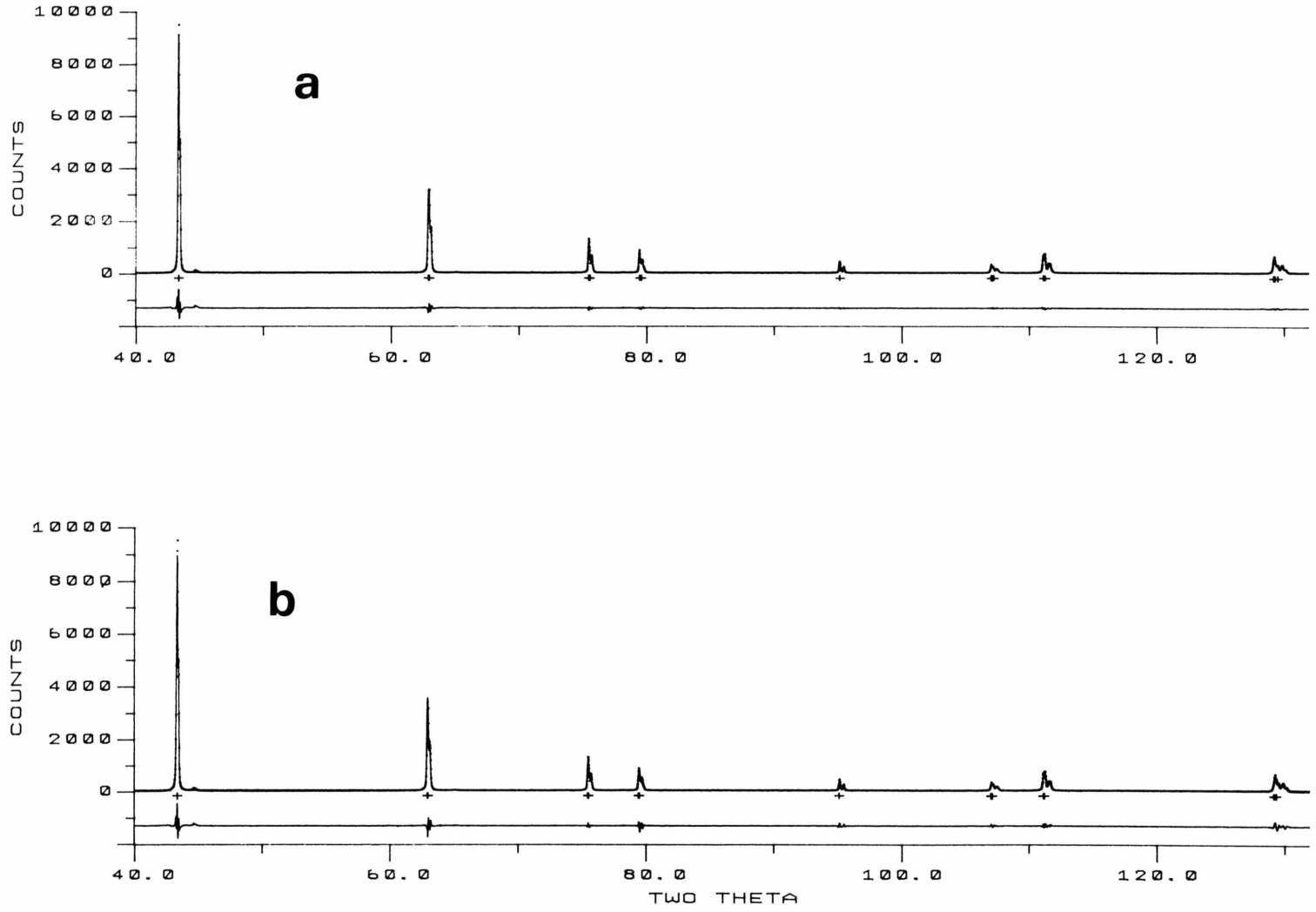

Fig. 2. Observed (markers) and calculated (continuous line) patterns obtained for a "bulk" sample. The calculated patterns a) and b) refer to the hexagonal models 1 and 2 of Table 1, respectively. The lower lines represent the difference between experimental and calculated.

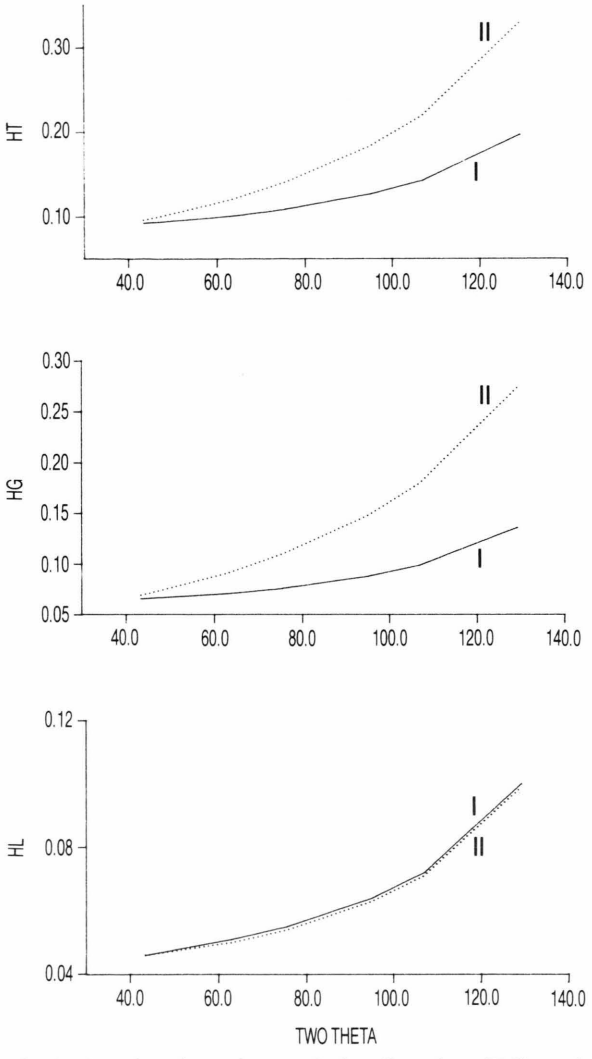

Fig. 3. Angular dependence of the Gaussian (HG) and Lorentzian (HL) components of the profile. The angular dependence of the total FWHM (HT) is also reported. $HG = (u\,\mathrm{tg}^2\,\Theta + w)^{1/2}$; $HL = y/\cos\Theta$. Continuous (I) and dotted (II) lines refer to models 1 and 2 of Table 1, respectively.

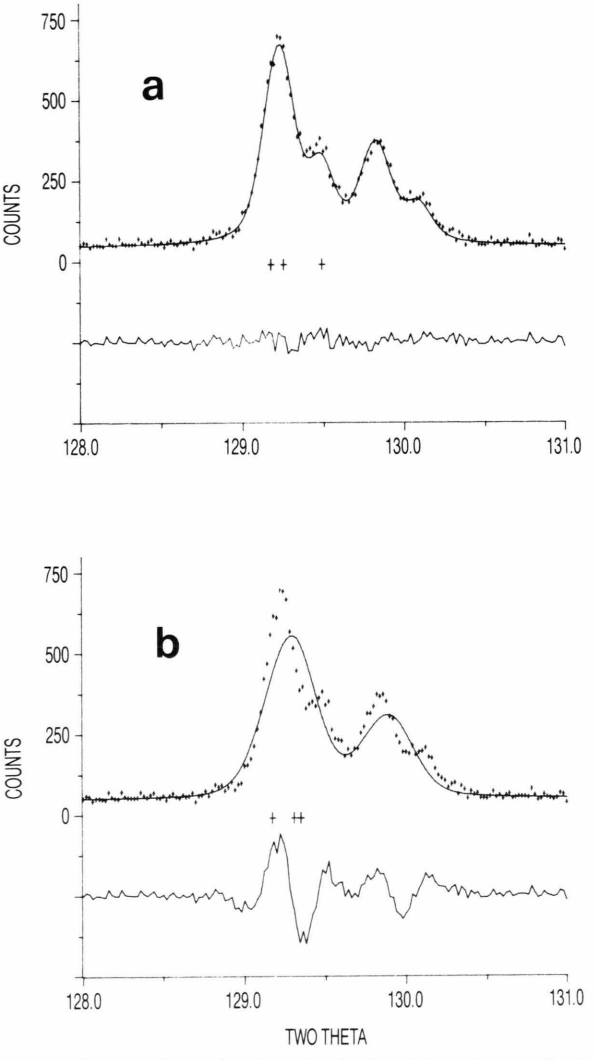

Fig. 4. Observed (markers) and calculated (continuous line) patterns of the "bulk" sample in the region of high angle reflexions: a) and b) refer to models 1 and 2 of Table 1, respectively.

lattice gives, together with the more favourable discrepancy factors, profile parameters by which the observed separation of the high angle reflexions can be explained. The conclusion can then be drawn that the structural distortion of the nickel oxide can be detected by the refinement of the structural and profile parameters of X-ray powder diffraction data.

3.2. Low Mass Samples

The results obtained for some of the refinements performed on low mass samples are reported in Table 2. Patterns were taken on samples of about 60, 30 and 15 mg, with step width of 0.02° and 0.03° and with filament current of 35 or 20 mA. The refinement procedure was exactly the same as for the bulk sample. The use of such different conditions of data collection aimed at verifying if and in which way experimental details can affect the results. As it can be seen, the major differences between the results of Table 2 and those obtained on the bulk sample (Table 1) concern the values of the thermal factors and of the zero error. The latter is higher while the former are lower than

Table 2. Refined parameters obtained by X-ray data collected under different conditions on low mass samples.

Sample mass/mg	60	60	60	30	15
Step width/°	0.02	0.02	0.03	0.03	0.03
Fil. current/mA	35	20	20	20	20
B (Ni)	0.1238	0.1054	0.1264	0.0601	−0.2441
	166	211	255	256	283
B (O)	0.2374	0.1349	0.1559	0.2032	0.1410
	477	593	717	741	864
Scale · 10^2	0.263	0.150	0.152	0.152	0.113
	14	10	12	12	11
u	0.00338	0.00285	0.00274	0.00289	0.00292
	33	39	47	45	48
w	0.00458	0.00420	0.00414	0.00512	0.00477
	18	22	26	28	30
y	0.04192	0.04236	0.04283	0.03931	0.03897
	96	124	150	141	164
$a=b$	2.95474	2.95459	2.95466	2.95456	2.95461
	2	3	3	3	3
c	7.22692	7.22672	7.22676	7.22664	7.22673
	8	10	12	12	13
Asymm.	0.98892	1.07552	0.99909	0.75847	0.63551
	8305	10888	13473	13057	16135
Zero	0.0780	0.0717	0.0753	0.0578	0.0685
	5	6	8	8	9
R_p	9.22	11.26	11.21	11.51	12.95
R_{wp}	12.42	15.74	15.56	15.72	16.91
R_E	11.11	14.63	14.63	14.42	15.24
GoF	1.25	1.16	1.13	1.19	1.23
D	1.77	1.77	1.77	1.76	1.79
R_B	2.43	2.93	3.10	3.23	5.73
R_F	1.50	1.89	1.99	1.79	3.08
c/a	2.44587	2.44593	2.44588	2.44593	2.44592
	9	12	13	13	13
$\sum y_i \cdot 10^{-6}$	0.3683	0.2120	0.1416	0.1456	0.1305
N	4549	4549	3033	3032	3032
Q	1.91	1.91	1.90	1.90	1.90

those obtained for the bulk sample. Moreover the thermal factor of the Ni atom appreciably decreases with decreasing sample mass and becomes negative for the sample of lowest mass (fifth column). It is noteworthy however, that the lattice parameters, and then the c/a ratio, are practically independent both of sample mass and experimental details, their values being practically identical to each other and to those obtained for the bulk sample. This is in favour of the applicability of the Rietveld refinement procedure to X-ray data collected on low mass samples. Also the profile parameters seem to allow a similar conclusion. As it can be seen in Fig. 5, they lead to calculated patterns which are able to explain the observed separation of the high angle reflexions.

It must be stressed, however, that the reliability of a refinement can be discussed from a quantitative point of view by analyzing its discrepancy factors. Among these the R_{wp} factor, which contains the quantity being minimized during the refinement, has long been considered the more suitable one to give information about the reliability of the refinement: but R_{wp} increases with decreasing pattern counts, so that it cannot be reliably used to compare the goodness of refinements performed on patterns collected under different experimental conditions. The lower value of R_{wp}, that the refinement of the first column of Table 2 presents over the other refinements reported in the same table, is due to the higher value of filament current which, in turn, resulted in an appreciably higher pattern count. When pattern counts are similar (first columns of Tables 1 and 2), the R_{wp} values are similar and, as expected, the lower R_{wp} value is obtained with the higher pattern count. It is now generally believed that the goodness of fit, defined as the square of the ratio between R_{wp} and R_E, represents the most suitable parameter to evaluate the reliability of a refinement. As it can be seen in Tables 1 (first column) and 2, the goodness of fit obtained for the bulk sample is sensibly higher than those for the low mass samples.

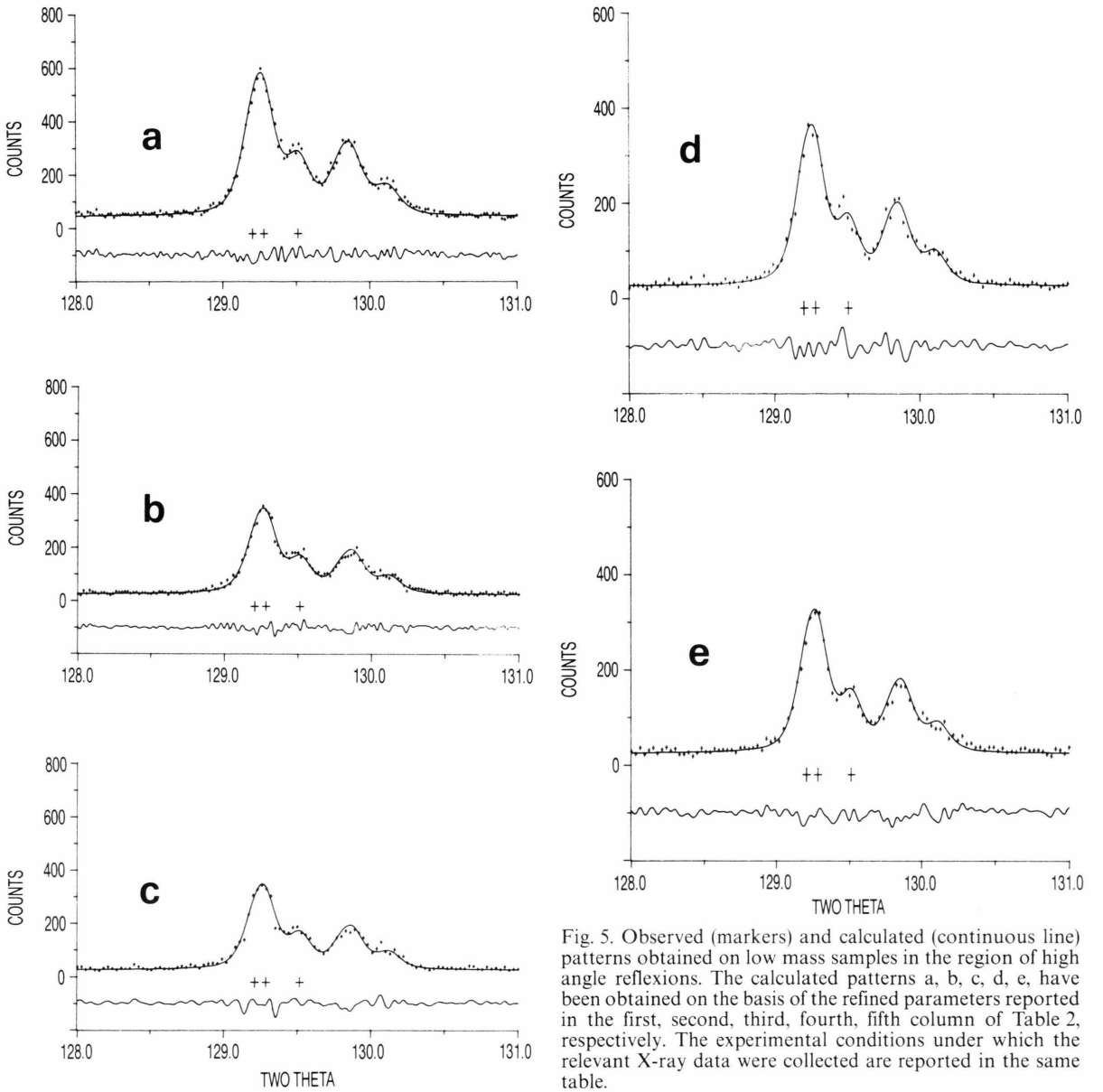

Fig. 5. Observed (markers) and calculated (continuous line) patterns obtained on low mass samples in the region of high angle reflexions. The calculated patterns a, b, c, d, e, have been obtained on the basis of the refined parameters reported in the first, second, third, fourth, fifth column of Table 2, respectively. The experimental conditions under which the relevant X-ray data were collected are reported in the same table.

The surprising conclusion should then be drawn that not only it is possible, but it is even better to apply the Rietveld refinement procedure to patterns collected on low mass samples rather than on bulk samples. Of course, it is quite difficult to believe that an increased sample mass can act as an intrinsic source of error, and it seems much more likely that the sample mass exerts only an apparent role on the goodness of fit. The problem then arises to thoroughly analyze in a critical way the influence of the experimental conditions. Such an analysis will be presented in a next work.

In fact, systematic studies already existing in the literature on the accuracy of the parameters and on the reliability of the e.s.d.'s obtained by Rietveld refinement [20], indicate that a correct choice of the conditions of data collection (step width and counting time) is of fundamental importance to avoid underestimation of the e.s.d.'s of the lattice parameters. Patterns were then collected at different step widths

Table 3. Refined parameters obtained by X-ray data collected under different step widths on "bulk" samples. Filament current: 20 mA; step counting time: 0.3 s.

Step width/°	0.02	0.03	0.05	0.10	0.15
B(Ni)	0.2602	0.2896	0.2912	0.2229	0.0080
	195	239	317	486	590
B(O)	0.1944	0.1410	−0.0009	0.3022	0.2551
	536	644	825	1200	1492
Scale · 10^2	0.202	0.204	0.204	0.202	0.179
	12	15	20	37	39
u	0.00343	0.00282	0.00332	0.00445	0.00265
	39	44	62	96	124
w	0.00369	0.00365	0.00382	0.00182	0.00426
	20	23	34	62	86
y	0.04402	0.04363	0.04328	0.04759	0.04490
	114	138	181	287	329
$a=b$	2.95410	2.95402	2.95420	2.95408	2.95392
	2	3	4	6	6
c	7.22537	7.22515	7.22554	7.22519	7.22492
	9	11	15	19	28
Asymm.	0.92122	0.74345	0.98894	1.26522	0.65529
	8742	11072	14254	20205	22308
Zero	0.0281	0.0253	0.0303	0.0271	0.0184
	6	7	9	15	21
R_p	10.77	10.80	10.89	9.64	10.20
R_{wp}	15.04	14.92	15.31	14.45	14.33
R_E	13.46	13.43	13.43	13.56	13.87
GoF	1.25	1.23	1.30	1.14	1.07
D	1.67	1.74	1.76	1.81	1.78
R_B	2.88	2.86	2.30	1.72	3.66
R_F	1.70	1.45	1.46	1.52	2.53
c/a	2.44587	2.44587	2.44585	2.44583	2.44587
	10	10	20	20	30
$\sum y_i \cdot 10^{-6}$	0.2509	0.1680	0.1008	0.04938	0.03144
N	4549	3033	1820	910	607
Q	1.91	1.90	1.87	1.82	1.79

both on bulk and on low mass samples in order to maximize the accuracy and precision of the lattice constants and to verify the influence, if any, of the step width on the goodness of fit. The results of the refinement performed on these patterns are reported in Tables 3 and 4. It can be seen that:

1) the goodness of fit changes with changing the step width and reaches a common minimum for step widths of 0.15° (bulk sample, Table 3) and 0.10° (low mass sample, Table 4);
2) when the goodness of fit is at a minimum, the e.s.d.'s of the lattice parameters reach their maximum, becoming three times (bulk sample) or two times (low mass sample) greater than at step widths of 0.02°;
3) the Durbin-Watson D coefficient, tested against the 0.1 significance point Q [21], indicates that, while the best refinement of the bulk sample contains a slight positive serial correlation between adjacent steps in the profile, no serial correlation is present on the best refinement of the low mass sample.

Thus, it is evident that the step width has a greater role than the sample mass. Such a role, together with those of other parameters, will be extensively discussed, as above noted, in a subsequent paper. It is, however, important to remark here that, when the appropriate step width is selected, practically the same (and the lowest) goodness of fit and the same lattice parameters and e.s.d.'s are obtained both on bulk and on low mass samples. While ruling out the idea that an increased sample mass might act as an intrinsic source of error, these results fully confirm that the Rietveld refinement procedure can be applied to perform reliable structural characterization of low mass samples.

4. Conclusions

The Rietveld analysis of X-ray data collected on NiO powders confirms the presence of a slight rhombohedral distortion in the NiO lattice. The refinement of the structural and profile parameters of the diffraction data collected both on bulk and on low mass samples

Table 4. Refined parameters obtained by X-ray data collected under different step widths on low mass samples (15 mg). Filament current: 20 mA; step counting time: 0.3 s. (The results obtained for step width = 0.03° have been reported in the last column of Table 2).

Step width/°	0.02	0.05	0.10	0.15
B (Ni)	−0.1688	−0.1503	−0.0930	−0.0311
	233	360	508	744
B (O)	0.0954	0.1042	0.2437	0.2364
	695	1070	1467	1927
Scale · 10^2	0.114	0.115	0.117	0.124
	09	14	20	36
u	0.00353	0.00432	0.00339	0.00234
	42	70	82	175
w	0.00457	0.00394	0.00335	0.00235
	24	38	63	98
y	0.03877	0.03897	0.03782	0.04872
	134	208	281	498
$a = b$	2.95455	2.95453	2.95446	2.95450
	3	4	6	8
c	7.22653	7.22645	7.22602	7.22587
	11	17	24	25
Asymm.	0.60765	0.32568	1.16673	0.50855
	14044	21774	32889	32070
Zero	0.0887	0.0850	0.0802	0.0828
	7	11	18	21
R_p	13.00	12.68	11.21	11.87
R_{wp}	17.04	16.64	15.73	16.66
R_E	15.36	15.35	15.31	15.23
GoF	1.23	1.18	1.06	1.20
D	1.74	1.74	1.93	1.87
R_B	6.81	6.61	4.21	4.72
R_F	3.71	3.68	3.00	2.73
c/a	2.44590	2.44589	2.44580	2.44572
	10	20	30	30
$\sum y_i \cdot 10^{-6}$	0.1928	0.07716	0.03874	0.02610
N	4549	1820	910	607
Q	1.91	1.87	1.82	1.79

leads to a lattice parameter ratio $c/a = 2.4458(3)$ which is in good agreement with the literature [11] value of 2.4456(7). This result allows one to state that the Rietveld refinement procedure can be reliably applied, irrespective of the sample mass, to evaluate the lattice parameters of nickel oxide (and possibly of related compounds).

Acknowledgement

This work has been supported by MURST 40% funds.

[1] E. J. S. Verwey, Semiconducting Materials, Butterworths, London 1951, p. 151.
[2] I. Bronsky and N. M. Tallan, J. Chem. Phys. **49,** 1243 (1968).
[3] V. B. Tase and J. B. Wagner, Jr., J. Appl. Phys. **54,** 6459 (1983).
[4] R. R. Heikes and W. D. Johnston, J. Chem. Phys. **26,** 582 (1957).
[5] S. Van Houten, J. Phys. Chem. Solids **17,** 7 (1960).
[6] K. Kuomoto, Z. T. Zhang, and H. Yaganida, Yogyo Kyokai Shi **92,** 83 (1984).
[7] J. B. Goodenough, D. G. Wickham, and W. J. Croft, J. Phys. Chem. Solids **5,** 107 (1958).
[8] EPRI, DOE/EPRI Workshop on MCFCs, Rep. no. WS-78-135, EPRI, Palo Alto, CA 1979.
[9] J. R. Selman and T. D. Claar, in: Molten Carbonate Fuel Cell Technology, Electrochem. Soc., Pennington, NJ 1982.
[10] K. Kinoshita, F. R. Larnon, and E. J. Cairns, Fuel Cells, a Handbook (DOE/METC-88/6096, 1988), Chapt. 4.
[11] H. P. Rooksby, Acta Cryst. **1,** 226 (1948).
[12] L. D. Dyer, B. S. Borie, Jr., and G. P. Smith, J. Amer. Chem. Soc. **76,** 1499 (1954).
[13] International Tables for X-Ray Crystallography, Vol. I A, D. Reidel, Dordrecht 1983, p. 14.
[14] H. M. Rietveld, J. Appl. Cryst. **2,** 65 (1969).
[15] D. B. Wiles and R. A. Young, J. Appl. Cryst. **14,** 149 (1981).
[16] International Tables for X-Ray Crystallography, Vol. IV, Kynok Press, Birmingham 1974, pp. 99, 149.
[17] E. Hovestreydt, Acta Cryst. **A 39,** 268 (1983).
[18] P. Thompson, D. E. Cox, and J. B. Hastings, J. Appl. Cryst. **20,** 79 (1987).
[19] I. C. Madsen and R. J. Hill, J. Appl. Cryst. **21,** 398 (1988).
[20] R. J. Hill and I. C. Madsen, J. Appl. Cryst. **19,** 10 (1986).
[21] R. J. Hill and H. D. Flack, J. Appl. Cryst. **20,** 356 (1987).